

Deformable Convolution Based Road Scene Semantic Segmentation of Fisheye Images in Autonomous Driving

Anam Manzoor¹, Aryan Singh¹, Ganesh Sistu¹, Reenu Mohandas¹, Eoin Grua¹, Anthony Scanlan¹, Ciarán Eising¹

¹Data-Driven Computer Engineering Group, Dept. of Electronic and Computer Engineering, University of Limerick

Abstract

This study investigates the effectiveness of modern Deformable Convolutional Neural Networks (DCNNs) for semantic segmentation tasks, particularly in autonomous driving scenarios with fisheye images. These images, providing a wide field of view, pose unique challenges for extracting spatial and geometric information due to dynamic changes in object attributes. Our experiments focus on segmenting the Wood-Scape fisheye image dataset into ten distinct classes, assessing the Deformable Networks' ability to capture intricate spatial relationships and improve segmentation accuracy. Additionally, we explore different loss functions to address class imbalance issues and compare the performance of conventional CNN architectures with Deformable Convolution-based CNNs, including Vanilla U-Net and Residual U-Net architectures. The significant improvement in mIoU score resulting from integrating Deformable CNNs demonstrates their effectiveness in handling the geometric distortions present in fisheye imagery, exceeding the performance of traditional CNN architectures. This underscores the significant role of Deformable convolution in enhancing semantic segmentation performance for fisheye imagery.

Keywords: Fisheye Images, Deformable Convolution, Semantic segmentation

1 Introduction

Semantic segmentation is indispensable in autonomous driving, as it enables precise object recognition and scene comprehension, essential for safe navigation [Divakarla et al., 2023]. By accurately labelling pixels in images, vehicles can perceive pedestrians, road lanes, and other critical elements in their surroundings, facilitating informed decision-making and boosting traffic safety. In autonomous driving, images acquired from multiple fisheye cameras positioned around the vehicle provide a comprehensive 360° view of the surroundings [Ramachandran et al., 2021] as shown in Figure 1.

Unlike conventional cameras, fisheye cameras provide broader scene coverage, which is particularly beneficial in navigating complex urban environments. Thus, integrating semantic segmentation with fisheye images enhances autonomous vehicles' capabilities, allowing them to interpret scenes and navigate adeptly across diverse driving scenarios accurately, as discussed in [Cho et al., 2023]. However, fisheye images often suffer from the loss of translation equivariance, necessitating specialized CNN architectures capable of effectively handling these translation transformations. Traditional CNN algorithms such as spherical CNNs [Cohen et al., 2018] and mapped CNNs [Eder et al., 2019] encounter challenges when applied to fisheye images due to their inherent radial distortion, requiring rectification before application. These rectification methods involve cubic and spherical mapping as illustrated in [Wang et al., 2018], [Cho et al., 2023], and [Hawary et al., 2020], respectively, aim to mitigate the effects of fisheye distortion. Yet, this rectification approach presents drawbacks such as resampling distortion artefacts

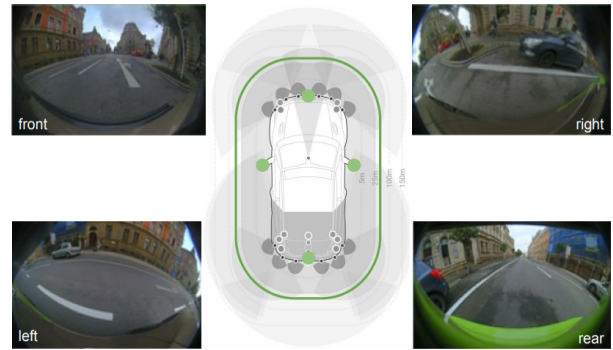


Figure 1: Four fisheye cameras mounted around the vehicle to provide complete 360-degree coverage.

and reduced field-of-view, highlighting the need for innovative solutions. Therefore, after exploring various CNN networks and hypothesizing potential solutions, recent advancements in Deformable Convolution Neural Networks have emerged as promising candidates. As introduced by [Dai et al., 2017], [Deng et al., 2019], and [Zhu et al., 2019], Deformable CNNs offer a compelling approach where the shape of the convolutional kernel is dynamically adjusted based on the object’s shape and position during training. This adaptability aligns well with the challenges posed by fisheye imagery, potentially enabling more efficient and accurate modelling of spatial relationships within distorted images.

Thus, our study primarily focuses on exploring the effectiveness of Deformable Convolutions as an alternative to regular convolutional layers in segmenting fisheye images using U-Net [Ronneberger et al., 2015]. We examine multi-view scene processing to assess the versatility of our approach. Additionally, we explore how incorporating images from various scenes can generalize the model to improve the segmentation accuracy while evaluating the effectiveness of different versions of the U-Net model. Rather than solely aiming for state-of-the-art results, we highlight the role of Deformable Convolutions in facilitating view-agnostic learning as discussed in [Shang et al., 2022], also shedding light on their intrinsic advantages for fisheye image segmentation. We also provide baseline results from the Woodscape dataset to validate our findings.

This paper starts by providing a thorough background study in Section 2, followed by an explanation of proposed methodologies for semantic segmentation of fisheye images in Section 3. Section 4 examines the outcomes from the implemented models, while Section 5 summarizes the paper’s conclusions and suggests future research directions.

2 Background Study on Semantic Segmentation in Automotive Imaging

A pioneering approach for image segmentation was using CNN networks. Semantic segmentation methods utilizing Convolutional Neural Networks distinguish themselves from other classical techniques owing to their capacity for end-to-end training and robust generalization to novel and limited data. CNNs also play a pivotal role by encapsulating prior knowledge regarding geometric transformations, facilitated by their adaptable model capacity and translational invariant properties, achieved through max-pooling layers within the network [Long et al., 2015]. With the widespread accessibility of high-performance Graphics Processing Units (GPUs) and intuitive deep learning frameworks, CNN-based models have achieved notable advancements across diverse domains, notably within semantic segmentation for autonomous driving [Huang and Chen, 2020], and [Xie et al., 2021].

The U-Net architecture, extensively utilized for tasks like semantic segmentation and image translation in computer vision, follows an encoder/decoder design with batch-normalization and ReLU activation functions after each convolution block, as detailed in [Ronneberger et al., 2015]. Additionally, the Residual U-Net, an evolved variant discussed in [Quan et al., 2021], incorporates residual blocks and internal long skip connections, along with extra operations between convolution blocks in the encoder and decoder paths, enhancing information flow and mitigating gradient vanishing issues. These architectures, known for their encoder-decoder design, efficiently extract features and generate segmentation maps. Skip connections help preserve spatial information for precise object localization, while the Residual U-Net’s integration of residual connections ensures robust network training. Overall, these frameworks excel in semantic segmentation tasks due to their efficient operations, adaptability, and capacity to capture both local and global contexts.

Fisheye cameras, commonly employed in autonomous driving, offer an expanded field of view compared to rectilinear images, capturing a broad spectrum of visual information. This inherent advantage makes fisheye cameras particularly valuable across diverse applications such as intelligent surveillance, drone technology [Yang et al., 2020], and autonomous driving [Kumar et al., 2021]. Nevertheless, its unique spherical view introduces significant distortions, where objects near the fisheye lens within a fisheye image exhibit considerable enlargement and distortion. At the same time, those farther away experience larger distortions due to low pixel density on the edges. As a result, the same object appears with different shapes at various positions within fisheye images, posing a unique challenge for the semantic segmentation task [Zhou et al., 2024].

The semantic segmentation of fisheye images using convolutional neural networks (CNNs) has presented unique challenges compared to rectilinear images. CNNs struggle with handling large-scale spatial transformations due to their fixed receptive fields within the network [Dai et al., 2017]. Thus, the optical distortions inherent in fisheye imagery impede CNNs’ ability to model unknown geometric transformations effectively. These distortions vary based on the object’s view angle relative to the camera, adding complexity to segmentation tasks. While various data augmentation techniques and synthetic data generation methods using regular CNNs have been explored, they often inadequately represent the complexities of real-world fisheye images [Sáez et al., 2018, Ye et al., 2020, Deng et al., 2017]. Therefore, training a model with raw fisheye data and applying semantic algorithms without undistortion could offer an optimal solution for building a generalized model. Furthermore, our literature review revealed a scarcity of publicly available fully annotated fisheye datasets for understanding road scenes. Only a few datasets, including OmniScape, [Sekkat et al., 2020], WoodScape [Yogamani et al., 2019], and SynWoodScape [Sekkat et al., 2022], provide semantic segmentation ground truths specifically designed for fisheye images.

The introduction of Deformable Convolution, followed by the advancements in modulated Deformable convolution introduced by [Dai et al., 2017] and [Zhu et al., 2019], respectively, has significantly enhanced the ability to handle geometric transformations in computer vision tasks. Modulated Deformable Convolution dynamically adapts to the dimensions and contours of detected objects, thereby enabling precise focus on relevant image regions. In contrast to conventional techniques using a fixed position kernel sampling, the deformable convolution introduces learned positional offsets to every sampled point of the kernel. This convolutional mechanism dynamically learns the perceptual field based on identified objects, significantly enhancing spatial sampling and producing robust and accurate feature representation. However, there has been limited exploration into harnessing Deformable Convolutions to address the challenge of learning unfamiliar geometric transformations in real-world fisheye imagery, especially within the automotive sector.

A recent study by [Cho et al., 2023] introduced a novel viewpoint augmentation technique, leveraging the Woodscape dataset to capture the distortion characteristics inherent in fisheye images. Furthermore, to our knowledge, only one recent study has compared regular CNNs with Deformable Convolutions for semantic segmentation of automotive fisheye images by deploying Residual U-Net [El Jurdi et al., 2023], demonstrating promising results in adapting to the unique characteristics of fisheye images with a single view, i.e., only Front view training and testing. To the best of our knowledge, the current literature has not explored the integration of the Deformable Convolutional component into the vanilla U-Net model for fisheye image segmentation, particularly in accommodating diverse viewpoints like Front View, Rear View, and Mirror Left and Right Views during both training and testing phases to enhance model generalization and performance.

3 Methodology

Our primary model builds upon the U-Net and Residual U-Net architectures proposed in [Ronneberger et al., 2015] and [Quan et al., 2021] respectively, incorporating Deformable Convolutions as discussed in [Deng et al., 2019]. We expand the model derived from the vanilla U-Net and Fully Residual U-Net architectures by substituting the traditional convolutional blocks with Deformable Convolutions. We focus on presenting only one variation with Deformable Convolution Blocks to limit the total number of experiments. Our primary contribution lies in modifying the initial and final convolutional layers of both the vanilla U-Net and Residual U-Net, as illustrated in Figure 2. This alteration enables the network to account for spatial and geometric characteristics during the training process [Deng et al., 2019]. Moreover, we explore different variants of the baseline U-Net network, namely V_U-Net, V_DeUNet, R_U-Net, and R_DeU-Net models.

3.1 Dataset

To evaluate our approach and establish a correlation between our model’s performance and the complexities inherent in fisheye imagery, we utilized the publicly available real-world WoodScape dataset introduced in [Yogamani et al., 2019]. This dataset consists of 10,000 annotated images captured from four different view

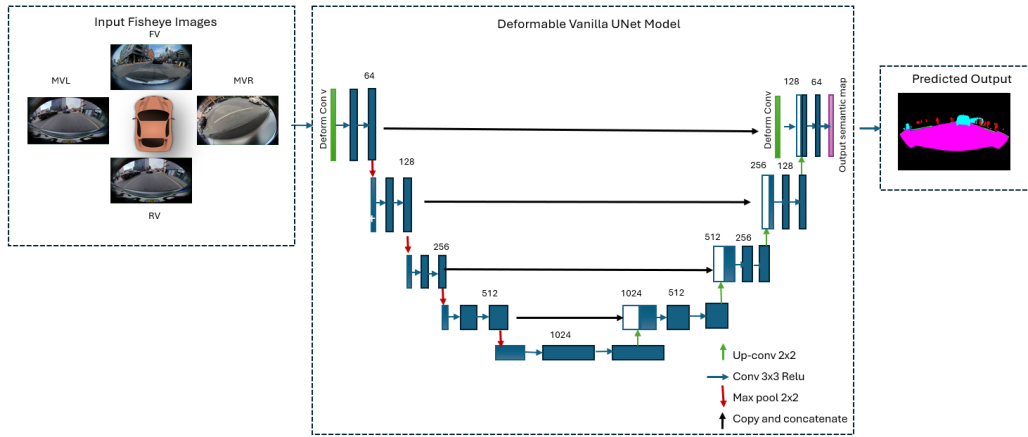


Figure 2: Baseline Vanilla DeU-Net model where Deformable Convolution block injected into the first layer of the encoder and last layer of decoder path to better account the spatial and geometric characteristics of fisheye images during training.

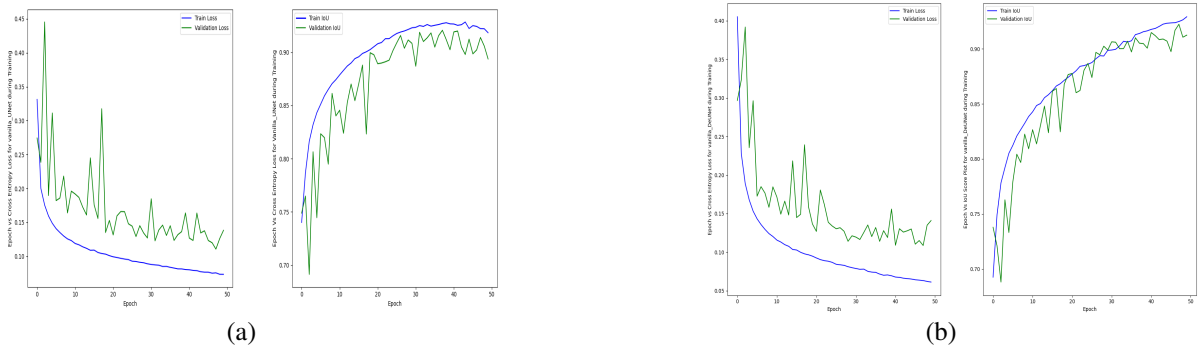


Figure 3: Epoch Vs Cross Entropy Loss and IoU score illustrated by Figures (a) and (b) showing the Epoch Vs Cross Entropy Loss and IoU score with Vanilla U-Net and Vanilla DeU-Net throughout the training process.

angles: Front View (FV), Mirror-View Right (MVR), Mirror-View Left (MVL), and Rear View (RV) of a vehicle. The dataset provides the semantic annotations for ten classes, including road, lane markings, curb, person, rider, car, bicycle, motorcycle, traffic sign, and background. Upon examining the dataset characteristics, it becomes apparent that a significant class imbalance exists concerning the occurrence of specific classes, such as bicycle, motorcycle, and traffic signs, which are less dominant than the road, landmarks, and curb courses across the entire image dataset.

3.2 Experimental Setup

To ensure reproducibility, we established an experimental framework. We implemented both the vanilla and Fully Residual U-Net model with and without Deformable convolution blocks referred to as V_U-Net (Vanilla U-Net), V_DeUNet (Vanilla Deformable U-Net), R_U-Net (Residual U-Net), and R_DeU-Net (Residual Deformable U-Net) models. Moreover, we explore the effectiveness of the Deformable U-Net model across the multi_view training and testing instead of a single view. We initially partitioned the datasets into training, validation, and test sets using an 80% , 10% , and 10% split, respectively. This split ensured that all views were uniformly distributed across the dataset partitions. The training was done from scratch using the PyTorch framework on an NVIDIA GeForce RTX 3080 GPU. We employed the Adam optimizer and initialized the weights randomly, selecting a batch size of 1 to facilitate rapid adaptation of the model to the dataset while mitigating the risk of overfitting to the limited training data and preventing memory errors. The training continued for 50 epochs without encountering any memory issues. The initial learning rate is set to 1×10^{-4} and adjusted according to the validation performance during training.

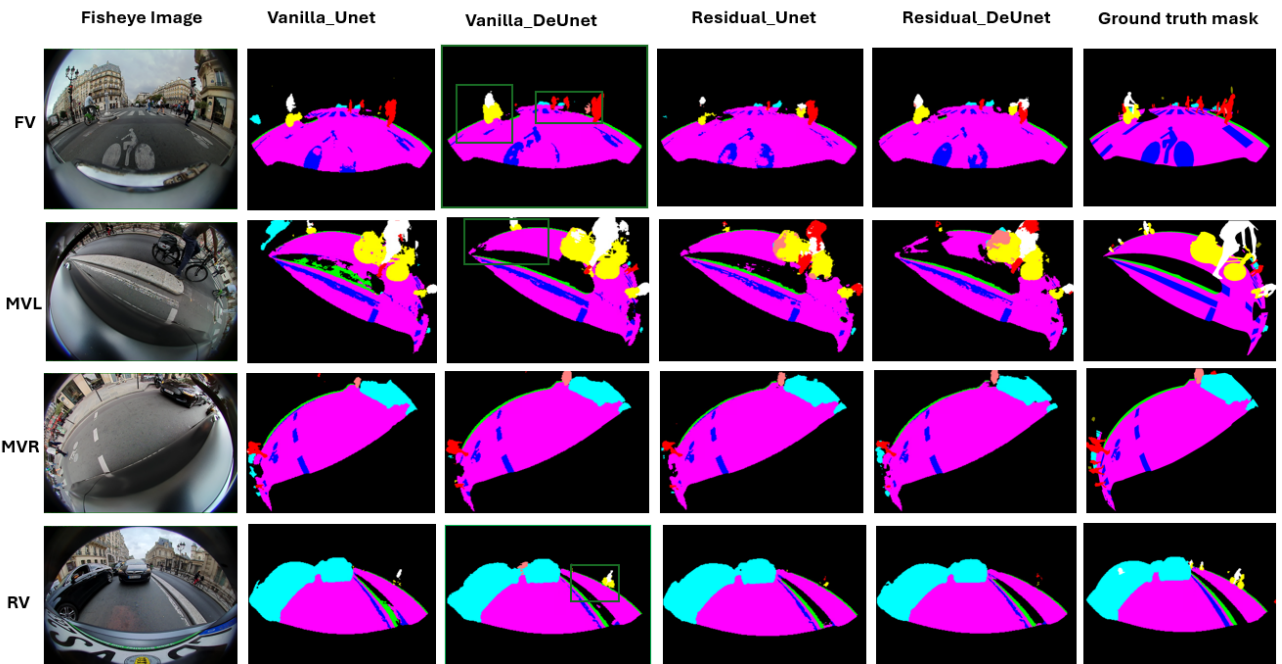


Figure 4: Visualizations of results on Woodscape fisheye images and corresponding ground truth masks are presented across baseline models including Vanilla_U-Net, Residual_U-Net, Deformable_U-Net, and Deformable_Residual model. Notably, the visualization performance with Vanilla_DeU-Net surpasses the other models, as indicated with green boxes compared to ground truth masks, with particular emphasis on distorted edges.

Moreover, to identify the most effective approach for handling the imbalanced dataset, we experimented with different variants of loss functions, including standard cross-entropy loss, focal loss, and class-weighted focal loss, calculated through a re-weighting scheme as discussed in [Paszke et al., 2016]. For pre-processing, we resized the RGB images to dimensions of 256x256 for computation efficacy. During training and validation, we applied augmentation techniques such as horizontal flipping (with a probability of 0.5) with random adjustments to brightness and contrast to improve the model’s generalization ability. Additionally, we normalized the pixel values of the images to ensure they fell within the range of 0 to 1 and transformed into tensors. The curves illustrating the Training and Validation Epoch versus Cross-Entropy Loss, as well as IoU scores, are depicted in Figure 3. All training curves are excluded due to space constraints. Finally, We evaluated the performance of the models on the test set annotations, which included all four side surround view images and masks, using both the mean Intersection over Union (mIoU) and accuracy metrics. The visualization results of four baseline models, Vanilla_U-Net, Vanilla_DeU-Net, Residual_U-Net, and Residual_DeU-Net, to assess the efficacy of Deformable convolutions on baseline models are shown in Figure 4.

4 Results and Experiments

Integrating Deformable blocks into the initial layers of the encoder and the final layer of the decoder paths of U-Net variants substantially improved class IoU scores and accuracy compared to the Vanilla and Residual U-Net baseline models. As discussed earlier, we utilized three different loss functions, cross-entropy loss, focal loss, and weighted focal loss, to explore their impact on model performance and the imbalanced dataset. The results, as summarized in Table 1, underscore the significance of our approach for fisheye datasets. To elaborate further, Table 1 initially presents the outcomes with the baseline Vanilla_U-Net_ce, outlining the IOU score for each class. Subsequently, upon integrating Deformable blocks into the baseline Vanilla_U-Net_ce (here, "ce" represents training with cross-entropy loss), notable enhancements in IOU scores for specific classes were observed: Curb by 0.01, Person by 0.11, Rider by 0.05, Bicycle by 0.001, Motorcycle by 0.01, and Traffic Sign by 0.10, respectively.

Similarly, when Deformable blocks were integrated into the Residual U-Net network, the IOU scores for each class outperformed those of the baseline Residual_U-Net. Furthermore, we explored the effectiveness of different loss functions, including standard and weighted focal loss, to address dataset imbalances. It is notable from Table 1 that only the IOU score of the Traffic Sign class improved by 0.14 compared to all other models. Our experiments reveal that standard cross-entropy loss is the most effective for training Deformable models on fisheye images. In addition, standard and weighted focal loss yielded promising results in handling dataset imbalances, as presented in 1. Specifically, the vehicle class achieved a 0.01 improvement in IoU score compared to Vanilla U-Net with standard focal loss. Similarly, with weighted focal loss, the traffic sign class improved by 0.27 and 0.14 in IoU score compared to Vanilla U-Net and Vanilla Deformable U-Net, respectively.

Moreover, the table demonstrates that integrating Deformable Convolutions into U-Net and Residual U-Net models enhances fisheye image segmentation. This underscores the adaptability of Deformable Convolutions to intrinsic fisheye characteristics and geometric transformations. Notably, the best results were achieved by V_DeU-Net_ce. Thus, by incorporating Deformable components into encoder and decoder layers, the model can better capture geometric distortions inherent in fisheye imagery and become robust towards camera position variations. Incorporating Deformable layers into the CNN network hinges on the dataset’s size. Enhancing the initial and final layers suffices large datasets to capture spatial and geometric distortion effectively. Conversely, exploring injections across various layers becomes necessary when dealing with smaller datasets. Training on a multi-view dataset has yielded promising results in our scenario, indicating the model’s robust performance. Hence, these experiments suggest the potential of deploying a Deformable model for fisheye image segmentation within computational constraints, opening up new avenues for research in this domain.

Table 1: The table presents class-specific accuracy and IoU scores for various configurations of Vanilla and Residual U-Net models, including their deformable versions, trained with different loss functions: cross-entropy (ce), standard focal loss (nwf), and weighted focal loss (wf). The highest IoU score for each class is highlighted in green for improved clarity.

Sr. #	Categories	V_U-Net_ce		V_DeU-Net_ce		V_DeU-Net_nwf		V_DeU-Net_wf		R_U-Net_ce		R_DeU-Net_ce		R_DeU-Net_wf	
		Acc ↑	IoU ↑	Acc ↑	IoU ↑	Acc ↑	IoU ↑	Acc ↑	IoU ↑	Acc ↑	IoU ↑	Acc ↑	IoU ↑	Acc ↑	IoU ↑
1	Background	0.98	0.96	0.99	0.97	0.99	0.96	0.98	0.95	0.98	0.95	0.98	0.96	0.97	0.94
2	Road	0.97	0.92	0.97	0.93	0.97	0.92	0.96	0.88	0.96	0.89	0.97	0.91	0.96	0.87
3	Lanemark	0.64	0.61	0.54	0.53	0.55	0.53	0.40	0.39	0.39	0.38	0.53	0.51	0.32	0.31
4	Curb	0.57	0.49	0.56	0.50	0.55	0.48	0.53	0.48	0.38	0.36	0.46	0.42	0.47	0.43
5	Person	0.28	0.23	0.37	0.32	0.34	0.27	0.29	0.23	0.04	0.04	0.15	0.12	0.27	0.19
6	Rider	0.44	0.41	0.54	0.46	0.42	0.36	0.51	0.44	0.18	0.16	0.17	0.15	0.10	0.10
7	Vehicles	0.91	0.84	0.90	0.85	0.90	0.85	0.87	0.76	0.89	0.73	0.88	0.81	0.84	0.67
8	Bicycle	0.60	0.52	0.74	0.53	0.49	0.43	0.47	0.38	0.33	0.28	0.45	0.37	0.07	0.06
9	Motorcycle	0.46	0.37	0.73	0.47	0.54	0.42	0.56	0.44	0.14	0.10	0.29	0.22	0.44	0.31
10	Traffic Sign	0.09	0.09	0.11	0.12	0.10	0.10	0.39	0.36	0.02	0.01	0.02	0.02	0.18	0.17
Average mIOU		0.93		0.93		0.91		0.88		0.89		0.89		0.85	
Average Accuracy		0.99		0.99		0.99		0.98		0.94		0.94		0.98	

5 Conclusion and Future Work

This study investigated the effectiveness of integrating Deformable Convolutions for semantic segmentation of fisheye images in the automotive domain. We explored four models as a baseline: Vanilla_U-Net, Residual_U-Net, Deformable_U-Net, and Deformable_Residual_U-Net. Our proposed approach illustrates the promising potential of Deformable Convolutions in effectively learning fisheye image characteristics. Through our experiments, we observed that integrating Deformable Convolutional blocks allows for more refined and efficient modelling of fisheye images. As a result, future research could explore incorporating these blocks into alternative backbone architectures or multitask networks to enhance the semantic segmentation for synthetic and real-world datasets. Furthermore, avenues for investigation may include tasks such as instance segmentation, detection, and optical flow estimation. Additionally, integrating patchwise mechanisms into the model to capture local and global information about object positions, shapes, or depth maps as constraints could enhance segmentation performance and mitigate challenges associated with class size imbalances within datasets. We can also integrate this network into a transformer-based architecture for future endeavours to achieve even better semantic segmentation results for the automotive industry.

Acknowledgments

This work was supported, in part, by the Science Foundation Ireland grant 13/RC/2094 P2 and co-funded under the European Regional Development Fund through the Southern & Eastern Regional Operational Programme to Lero - the Science Foundation Ireland Research Centre for Software (www.lero.ie).

References

- [Cho et al., 2023] Cho, J., Lee, J., Ha, J., Resende, P., Bradai, B., and Jo, K. (2023). Surround-view fisheye camera viewpoint augmentation for image semantic segmentation. *IEEE Access*.
- [Cohen et al., 2018] Cohen, T. S., Geiger, M., Köhler, J., and Welling, M. (2018). Spherical cnns. *arXiv preprint arXiv:1801.10130*.
- [Dai et al., 2017] Dai, J., Qi, H., Xiong, Y., Li, Y., Zhang, G., Hu, H., and Wei, Y. (2017). Deformable convolutional networks. In *Proceedings of the IEEE International Conference on Computer Vision (ICCV)*.
- [Deng et al., 2019] Deng, L., Yang, M., Li, H., Li, T., Hu, B., and Wang, C. (2019). Restricted deformable convolution-based road scene semantic segmentation using surround-view cameras. *IEEE Transactions on Intelligent Transportation Systems*, 21(10):4350–4362.
- [Deng et al., 2017] Deng, L., Yang, M., Qian, Y., Wang, C., and Wang, B. (2017). Cnn based semantic segmentation for urban traffic scenes using fisheye camera. In *2017 IEEE Intelligent Vehicles Symposium (IV)*, pages 231–236. IEEE.
- [Divakarla et al., 2023] Divakarla, U., Bhat, R., Madagaonkar, S. B., Pranav, D., Shyam, C., and Chandrashekar, K. (2023). Semantic segmentation for autonomous driving. In *Information and Communication Technology for Competitive Strategies (ICTCS 2022) Intelligent Strategies for ICT*, pages 683–694. Springer.
- [Eder et al., 2019] Eder, M., Price, T., Vu, T., Bapat, A., and Frahm, J.-M. (2019). Mapped convolutions. *arXiv preprint arXiv:1906.11096*.
- [El Jurdi et al., 2023] El Jurdi, R., Sekkat, A. R., Dupuis, Y., Vasseur, P., and Honeine, P. (2023). Fully residual unet-based semantic segmentation of automotive fisheye images: a comparison of rectangular and deformable convolutions. *Multimedia Tools and Applications*, pages 1–23.
- [Hawary et al., 2020] Hawary, F., Maugey, T., and Guillemot, C. (2020). Sphere mapping for feature extraction from 360 fish-eye captures. In *2020 IEEE 22nd International Workshop on Multimedia Signal Processing (MMSP)*, pages 1–6. IEEE.
- [Huang and Chen, 2020] Huang, Y. and Chen, Y. (2020). Survey of state-of-art autonomous driving technologies with deep learning. In *2020 IEEE 20th International Conference on Software Quality, reliability and Security Companion (QRS-C)*, pages 221–228. IEEE.
- [Kumar et al., 2021] Kumar, V. R., Yogamani, S., Rashed, H., Sitsu, G., Witt, C., Leang, I., Milz, S., and Mäder, P. (2021). Omnidet: Surround-view cameras based multi-task visual perception network for autonomous driving. *IEEE Robotics and Automation Letters*, 6(2):2830–2837.
- [Long et al., 2015] Long, J., Shelhamer, E., and Darrell, T. (2015). Fully convolutional networks for semantic segmentation. In *Proceedings of the IEEE conference on computer vision and pattern recognition*, pages 3431–3440.
- [Paszke et al., 2016] Paszke, A., Chaurasia, A., Kim, S., and Culurciello, E. (2016). Enet: A deep neural network architecture for real-time semantic segmentation. *arXiv preprint arXiv:1606.02147*.

- [Quan et al., 2021] Quan, T. M., Hildebrand, D. G. C., and Jeong, W.-K. (2021). Fusionnet: A deep fully residual convolutional neural network for image segmentation in connectomics. *Frontiers in Computer Science*, 3:613981.
- [Ramachandran et al., 2021] Ramachandran, S., Sistu, G., McDonald, J., and Yogamani, S. (2021). Wood-scape fisheye semantic segmentation for autonomous driving—cvpr 2021 omniv workshop challenge. *arXiv preprint arXiv:2107.08246*.
- [Ronneberger et al., 2015] Ronneberger, O., Fischer, P., and Brox, T. (2015). U-net: Convolutional networks for biomedical image segmentation. In *Medical image computing and computer-assisted intervention—MICCAI 2015: 18th international conference, Munich, Germany, October 5-9, 2015, proceedings, part III 18*, pages 234–241. Springer.
- [Sáez et al., 2018] Sáez, A., Bergasa, L. M., Romeral, E., López, E., Barea, R., and Sanz, R. (2018). Cnn-based fisheye image real-time semantic segmentation. In *2018 IEEE Intelligent Vehicles Symposium (IV)*, pages 1039–1044. IEEE.
- [Sekkat et al., 2022] Sekkat, A. R., Dupuis, Y., Kumar, V. R., Rashed, H., Yogamani, S., Vasseur, P., and Honeine, P. (2022). Synwoodscape: Synthetic surround-view fisheye camera dataset for autonomous driving. *IEEE Robotics and Automation Letters*, 7(3):8502–8509.
- [Sekkat et al., 2020] Sekkat, A. R., Dupuis, Y., Vasseur, P., and Honeine, P. (2020). The omniscap dataset. In *2020 IEEE International Conference on Robotics and Automation (ICRA)*, pages 1603–1608. IEEE.
- [Shang et al., 2022] Shang, J., Das, S., and Ryoo, M. (2022). Learning viewpoint-agnostic visual representations by recovering tokens in 3d space. *Advances in Neural Information Processing Systems*, 35:31031–31044.
- [Wang et al., 2018] Wang, Y., Cai, S., Li, S.-J., Liu, Y., Guo, Y., Li, T., and Cheng, M.-M. (2018). Cubemap-slam: A piecewise-pinhole monocular fisheye slam system. In *Asian Conference on Computer Vision*, pages 34–49. Springer.
- [Xie et al., 2021] Xie, E., Wang, W., Yu, Z., Anandkumar, A., Alvarez, J. M., and Luo, P. (2021). Segformer: Simple and efficient design for semantic segmentation with transformers. *Advances in neural information processing systems*, 34:12077–12090.
- [Yang et al., 2020] Yang, L., Hu, G., Song, Y., Li, G., and Xie, L. (2020). Intelligent video analysis: A pedestrian trajectory extraction method for the whole indoor space without blind areas. *Computer Vision and Image Understanding*, 196:102968.
- [Ye et al., 2020] Ye, Y., Yang, K., Xiang, K., Wang, J., and Wang, K. (2020). Universal semantic segmentation for fisheye urban driving images. In *2020 IEEE International Conference on Systems, Man, and Cybernetics (SMC)*, pages 648–655. IEEE.
- [Yogamani et al., 2019] Yogamani, S., Hughes, C., Horgan, J., Sistu, G., Varley, P., O’Dea, D., Uricár, M., Milz, S., Simon, M., Amende, K., et al. (2019). Woodscape: A multi-task, multi-camera fisheye dataset for autonomous driving. In *Proceedings of the IEEE/CVF International Conference on Computer Vision*, pages 9308–9318.
- [Zhou et al., 2024] Zhou, J., Yang, D., Song, T., Ye, Y., Zhang, X., and Song, Y. (2024). Improved yolov7 models based on modulated deformable convolution and swin transformer for object detection in fisheye images. *Image and Vision Computing*, page 104966.
- [Zhu et al., 2019] Zhu, X., Hu, H., Lin, S., and Dai, J. (2019). Deformable convnets v2: More deformable, better results. In *Proceedings of the IEEE/CVF Conference on Computer Vision and Pattern Recognition (CVPR)*.